Fatigue evaluation on headed stud connectors with toe-plate failure mode using hot spot stress approach

Liu, Rong; Zhao, Hao; Feng, Zhiqiang; Xin, Haohui; Liu, Yuqing

DOI
10.1016/j.engfailanal.2020.104972

Publication date
2020

Document Version
Final published version

Published in
Engineering Failure Analysis

Citation (APA)
Liu, R., Zhao, H., Feng, Z., Xin, H., & Liu, Y. (2020). Fatigue evaluation on headed stud connectors with toe-plate failure mode using hot spot stress approach. *Engineering Failure Analysis*, *117*, Article 104972. https://doi.org/10.1016/j.engfailanal.2020.104972

Engineering Failure Analysis 117 (2020) 104972

Contents lists available at ScienceDirect

Engineering Failure Analysis

journal homepage: www.elsevier.com/locate/engfailanal

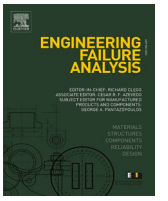

Fatigue evaluation on headed stud connectors with toe-plate failure mode using hot spot stress approach

Rong Liu [a], Zhao Hao[a], Feng Zhiqiang[a], Xin Haohui[b,c,*], Liu Yuqing[d]

[a] College of Civil and Transportation Engineering, Hohai University, Nanjing 210098, China
[b] Department of Civil Engneering, School of Human Settlements and Civil Engineering, Xi'an Jiaotong University, Xi'an, China
[c] Faculty of Civil Engineering and Geosciences, Delft University of Technology, Delft 2600AA, the Netherlands
[d] Department of Bridge Engineering, Tongji University, Shanghai 200092, China

ARTICLE INFO

Keywords:
Stud connectors
Toe-base crack
Fatigue strength
Hot spot stress
Finite element analysis

ABSTRACT

The headed stud connectors are widely used in a variety of innovative engineering applications of the infrastructure sector. The fatigue life of headed studs is significantly affected by the residual stress introduced from welding procedures. It is very important to develop a reliable numerical method to predict the fatigue performance of headed stud connectors. In this paper, the efficiency of fatigue life prediction, using the nominal stress (NS) and the hot spot stress (HSS) methods based on finite element simulation, is compared. The limitation using the NS method to predict the fatigue life of studs is discussed in this paper. The efficiency of the HSS analysis technique is validated by the fatigue test results in the literature.

1. Introduction

Headed stud shear connectors [38] are typically applied at the steel–concrete interface of composite beams to connect steel girders and the concrete slabs. Owing to its convenient welding procedures and the well-accepted mechanical behavior, the headed stud connectors remain dominant in the construction of modern steel–concrete composite structures, such as buildings, and bridges, etc. In terms of application in bridge engineering, the ever-growing traffic flow and the frequently reported overload cases call attention to the fatigue life evaluation to ensure the service quality of steel and concrete components.

The studs are generally welded to the base plates of steel members. Due to geometric discontinuity, the stud-plate welded joint (SPJ) suffers from the stress concentration due to external loads, and the secondary load effects caused by concrete shrinkage and creep. In addition, the fatigue life is significantly affected by the residual stress introduced by welding procedures [34]. The heat-affected zone (HAZ), as shown in Fig. 1, between the studs and base plates will reduce the fatigue life due to coexisting intrinsic defaults, such as micro-crystal dislocation, the meso-scope notch and the remarkable residual stress [14]. Type A is that the initial crack of the stud shank near the root is generated and gradually expands due to variable shear force, and finally fatigue failure occurs. Type B is due to insufficient welding quality, leading to local stress concentration and increased initial micro-cracks, so the stiffness of the interface between the stud and weld toe is low that the weld toe is torn under fatigue load. When the ratio of the diameter of the stud to the thickness of the steel plate is large, the steel plate becomes a weak part. Under the action of fatigue load, the steel plate crack at the weld toe propagates along the plate thickness direction and causes Type C failure [26][27]. As a result, the fatigue performance of SPJ draws a lot of attention from both academic and industry field. The toe-plate crack is one of the probable fatigue damages in SPJ

* Corresponding author.
E-mail address: H.Xin@tudelft.nl (H. Xin).

https://doi.org/10.1016/j.engfailanal.2020.104972
Received 19 June 2020; Received in revised form 29 August 2020; Accepted 27 September 2020
Available online 30 September 2020

[10,9]. It initiates at the weld toe and propagates through the base plate thickness. This paper focuses on fatigue life evaluation of headed studs with the toe-plate crack (Type B in Fig. 1).

Two procedures should be conducted regarding the fatigue life evaluation of SPJ. One is the empirical equation to predict the fatigue life in terms of the governing stress component at the potential crack section. The other is the effective numerical or analytical method to determine the threshold of the governing stress component, namely fatigue strength. For engineering application, the NS range is majorly used in fatigue design because it is convenient to be obtained by hand calculation. And the corresponding fatigue strength is determined according to series of fatigue tests for the [40] same structural detail [1,25,29,30,39]. Most of the contemporary design codes follow the methodology of NS method, like AASHTO LRFD [2], Eurocode [7], JSCE [17] and JTG [18].

Nevertheless, the traditional uses of studs in composite beams are widely extended, including composite joints [22], anchorage zones [23], Flange of steel I-shaped girder with corrugated web [11] and orthotropic steel decks with concrete overlays [5]. It is too complicated to determine NS for the extended applications with complex geometries due to lack of hand calculation formulas. Besides, the headed studs are under multiaxial stress status for the irregular structural details. The application scope of the NS method needs to be discussed because the nominal fatigue strength from uniaxial push-out tests may not well describe the multiaxial fatigue performance. Furthermore, the fatigue tests to determine the fatigue strength of non-standard studs are costly and time-consuming. Finally, the NS method could not predict the fatigue life of new connectors using advanced materials, such as rubber sleeved studs [36,37], resin-covered studs [32], and ultra-high-performance-concrete (UHPC) embraced studs [12].

Some scholars have used the hot spot stress method to estimate the fatigue life of key welded steel details of a railway composite bridge under the effect of dynamic load [31]. Fatigue behavior of the newly developed studs and the extended applications are of research interests and further advanced analysis techniques are required. The HSS method might be an alternative to the NS method when evaluating the non-standard studs. Two assumptions are followed when using the HSS method to evaluate the fatigue behavior of stud connectors. The first is that the studs hold nearly the same strength if equal structural stress ranges are applied at the hot spots, since these studs sharing the same welding technique and the same welding effects. The second is that the structural factors without considering welding effects could be explicitly included in HSS analysis models. As to butt weld and fillet weld, the guidelines for HSS calculation and the corresponding fatigue strength are suggested by the International Institute of Weld (IIW) [16]. HSS method has an explicit stress calculation and FE modeling guidelines. As a result, the analysis results ought to be reproducible. The method is also followed to evaluate the fatigue performance of orthotropic steel bridge decks [21,24].

With the development of computing capacity, refined solid FE models are often used to study the static and fatigue behavior of studs [6,28,20]. Regarding the geometric and mechanical differences between SPJ and the fillet/butt welded joints in steel structures, the hot spot stress calculation schemes needed to be further discussed to predict the fatigue life of headed studs. Moreover, the drawn-arc stud welding technique is somehow distinct from the fillet/butt welding concerning electric current, plunge-formed weld collar, and residual stress. Thus, the residual stress effects on fatigue life of butt welds/fillet welds [33] could not be directly applied to the fatigue life prediction of headed connectors, and welding effects on the fatigue strength of stud connectors should be further discussed by comparing the prediction with the fatigue test results.

This paper aims to illustrate the cases beyond the scope of the available specifications based on NS, especially for the innovative studs. The corresponding fatigue strength is determined by the regression of test results reported in the literature. The HSS method to predict the fatigue life of headed studs are illustrated in this paper.

2. Details of push-out specimen

Push-out specimens are recommended by Eurocode 4 (CEN 2004) [8] to determine the mechanical behavior of headed studs by static and fatigue tests. The push-out specimen used by Hirokazu [15] is referred to as the basic model in this paper. Geometric details

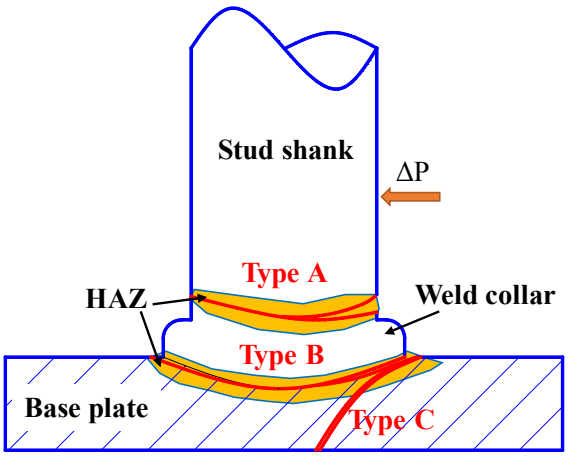

Fig. 1. Fatigue failure modes of welded studs.

are shown in Fig. 2. The width and thickness of concrete slabs are 540 mm and 150 mm, respectively. The diameter of rebars embedded in the slabs is 12 mm. The H-shape steel beam is composed of an 11 mm thickness flange and a 7 mm thickness web. The diameter of studs is 19 mm and the height of studs is 100 mm. Distance between the studs welded on the same flange is 120 mm.

3. Finite element models

Due to the symmetry of the push-out specimen, the 1/4 solid FE model with headed studs is built using the software ANSYS 14.0

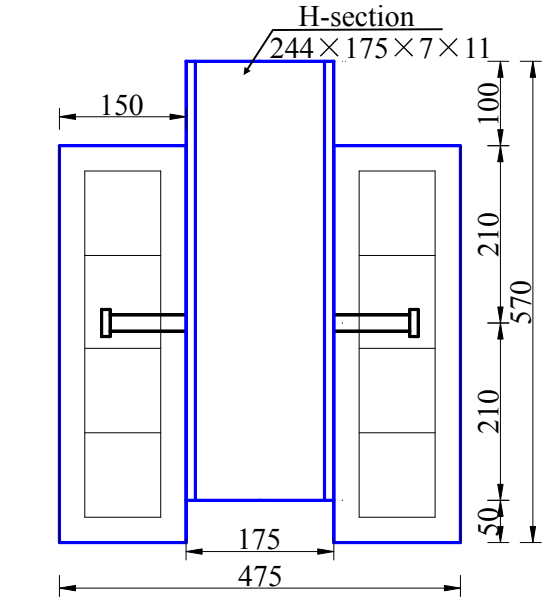

(a) Side view

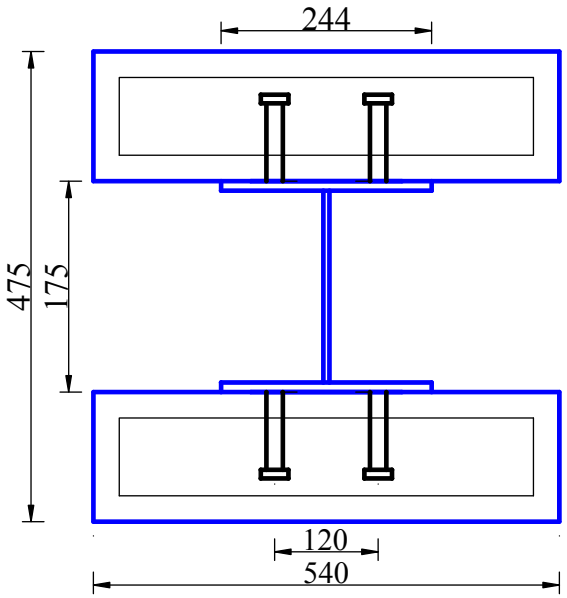

(b) Top view

Fig. 2. Geometry of push-out test specimen (unit: mm).

[4], see Fig. 3. The solid element SOLID185 is used to represent the steel beam, the studs, and the concrete slabs. The elements TARGET170 and CONTA174 are used to represent the steel–concrete contact behavior at the interface. BEAM188 is used for modeling of rebars.

The element size of the concrete slab and steel beam near SPJ is 10 mm. Sub-model technology is used to refine the local zone of SPJ. The minimum size is about 0.5 mm. The convergence of the stress results will be checked in this paper.

Young's modulus E_s of steel and studs is 2×10^5 MPa and E_c of concrete is 3.5×10^4 MPa. Poisson's ratio is 0.3 for steel and 0.16 for concrete respectively. The friction coefficient between stud and concrete is 0.3. Rigid restraints are applied to the bottom of the concrete slab and symmetrical restraints are applied to the symmetric surface. The push-out load was uniformly applied on the top cross-section of the steel beam using nodal forces.

4. Results and discussion

4.1. Limitation of NS method

4.1.1. Eccentricity effects

Although the base metals of SPJs are subjected to nearly the same nominal stresses, they may endure increasing local stresses if the studs are welded towards the edges of steel beams. To quantify the SCF of the plate, the nominal stress is calculated "force to steel beam cross-section" rather than "force to headed stud cross-section". With the variation of stud location, the stress concentration factor (SCF) K_b of the base metal is shown in Fig. 4. $K_b = \sigma_Y/\sigma_n$, where σ_n is the NS of the base metal along the Y-axis and it can be determined by Eq. (1). On the surface of the welding studs, the normal stress component σ_Y along Y-axis is the local stress from FE. Away from the centerline of the base metal, if the deviation of the stud location increases $6t_b$ from its original location, K_b increases 20%. On the contrary, the corresponding NS remains constant since the cross-sectional area A_b and the applied push out load P_Y are the same in the two cases. The results imply that NS methods (average shear stress) could not consider the local stress concentration effects caused by the eccentricity. However, the local stress concentration plays a dominant role in the determination of the fatigue performance of SPJ. Otherwise, the fatigue life of SPJ might be overestimated following the simplified NS method.

$$\sigma_n = P_Y/A_b \tag{1}$$

where P_Y is the push out load and A_b is the area of steel beam.

4.1.2. Stud spacing effects

The K_b distribution near the weld toe is shown in Fig. 4(b) when the width of the flange is reduced by $3t_b$. The stud spacing is corresponding to the width of the flange plate in the push-out tests. When the width of the flange plate is decreased, the stress distribution remains unchanged basically. This indicates that the change of flange plate width does not affect the stress distribution near SPJ. However, the fatigue life of headed studs with toe-plate failure mode is determined by the normal stress of steel plates based on the NS methods in the standard. The flange plate width decreases, and the cross-sectional area of steel beams decrease, leading to the increasing NS when the external force remains unchanged. The width of flange decreases by $3t_b$ and the NS increases by about 34%.

If the fatigue strength of weld toe is evaluated according to NS, when the width of flange decreases, the NS amplitude increases and the fatigue life decreases. However, the stress near the weld toe remains unchanged, that is, the fatigue life will not be greatly affected. Therefore, the NS method could not effectively consider the stud spacing effects in terms of toe-plate failure mode.

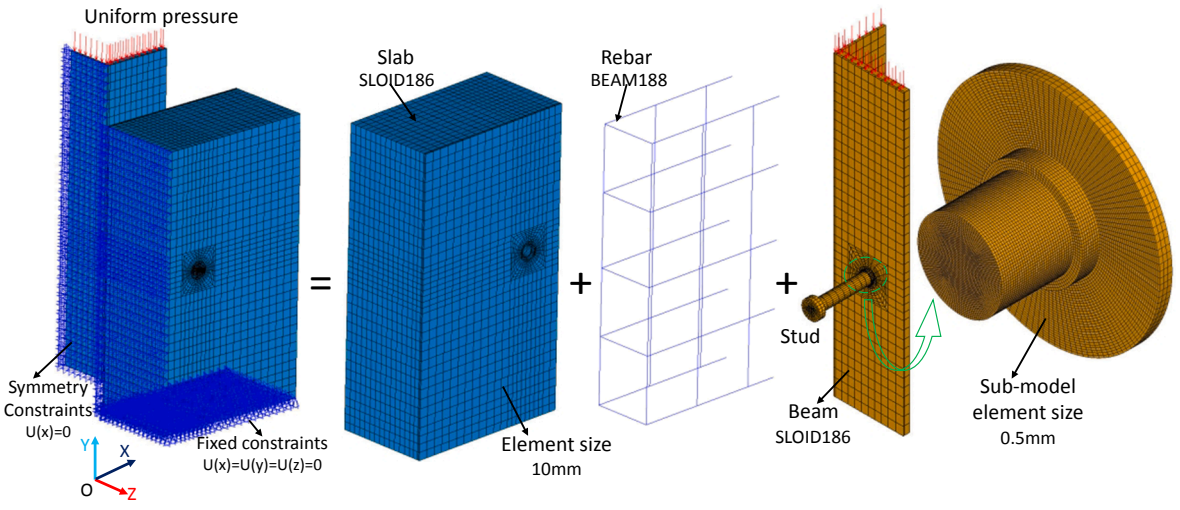

Fig. 3. Mesh and boundary of finite element model.

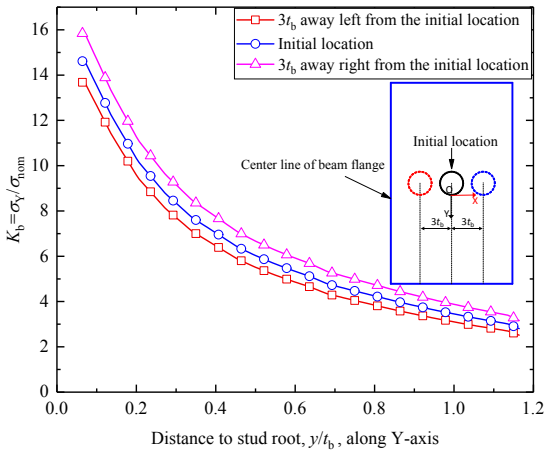

(a)Variation of stud location

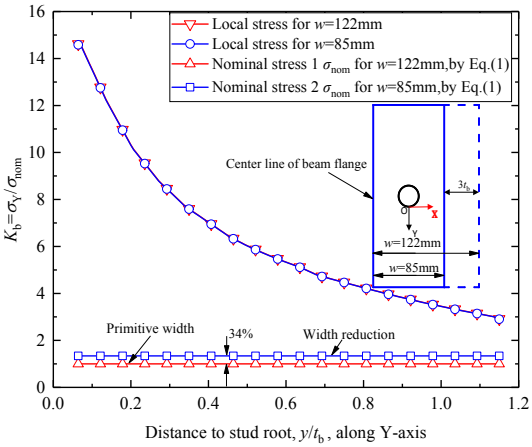

(b) Variation of flange width

Fig. 4. Local stress distribution with geometric variation.

4.1.3. *Concrete creep effects*

The local stress distribution of SPJ is dependent upon the creep behavior of the concrete slab, as shown in Fig. 5. Assuming that the initial loading age is 7 days and the applied load lasts for 10 years, the creep coefficient is calculated by ACI [3], the final creep coefficient is about 2.5. Based on the stress–strain equivalence idea that concrete creep is similar to metal creep, the Creep criterion of metal in ANSYS general FE program is used to simulate the creep effect of concrete. K_b at 0.4t_b away from the weld toe might increase 20% compared with the initial stage. The time-dependent behavior is also reported by previous studies [40]. The results showed that the stress redistribution of studs induced by concrete creep effects will reduce the fatigue life of headed studs. The increased local stress by the creep of concrete promotes the mean stress σ_m and the stress ratio R. Basically, σ_m and R are very important parameters for fatigue evaluation of welded structures.

The creep effects on fatigue behavior of SPJs is significant for long-span composite bridges, because of larger dead load and increasing traffic flows full of heavy trucks. However, the conventional NS method is difficult to include the time-dependent effects. The fatigue details classification of SPJs in current design specifications has not covered the time-dependent effects. It recommended that the time-dependent effects should be considered in the future fatigue life evaluation of headed studs.

4.1.4. *Effects of material plasticity*

When both steel and concrete are elastic or elastic–plastic materials, the distribution trend of K_b near the weld toe under different shear amplitudes is shown in Fig. 6. The ultimate shear capacity of the 19 mm stud in C50 concrete is about 128 kN, and the range of elastic bearing capacity is about 0–65 kN. When the loading force is 40 kN, the material plasticity does not affect the stress distribution near SPJ. As the loading force is 100 kN, the K_b at SPJ increases by about 18.5% compared with the full elastic material. The results show that the stress does not increase linearly with the increase of the load after the material enters the plasticity, thereby reducing the tendency of concentrated stress to increase.

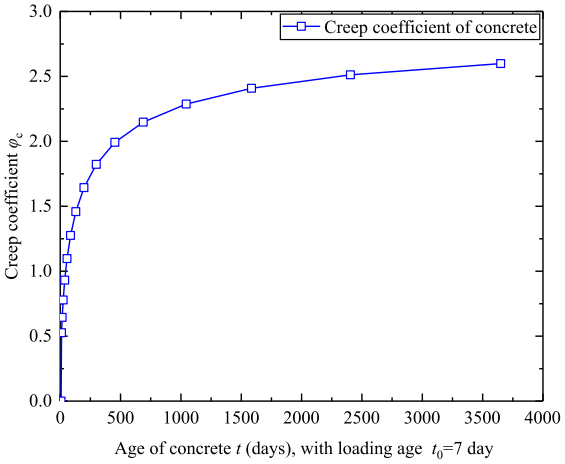

(a) Creep coefficient of concrete slab

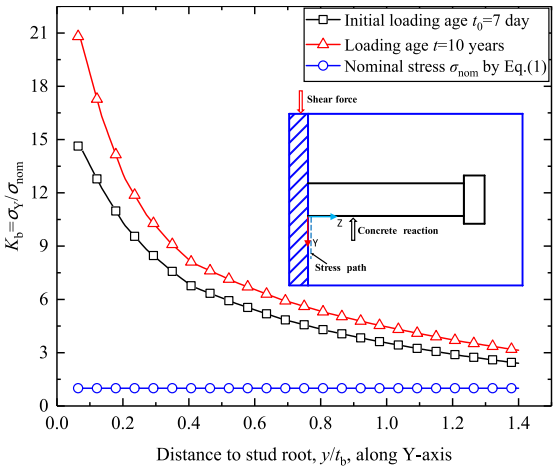

(b) Variation of loading time

Fig. 5. Local stress distribution with loading time variation.

Under the action of the trainload, the maximum shear amplitude of studs in the composite beam bridge is about 20 kN [20]. In most structures, the shear force of stud is basically in the linear stage of load slip curve, and the stress distribution near SPJ can also be accurately simulated by using fully elastic materials model, while the stress near SPJ predicted by the NS method is relatively low. When part of the components enters plasticity, the calculation using completely elastic material model compared with plastic material model can evaluate the fatigue life of the structure more safely, which is beneficial to the safe operation of the structure.

4.1.5. Effects of contact stiffness relaxation

To minimize the tensile stresses induced by shrinkage of concrete slabs, the studs with relaxed initial contact stiffness are usually used. Among them, the rubber sleeved stud is a recently reported type for application in composite bridges [37,36]. In this paper, the thickness of the rubber sleeve is 2.5 mm, the height is 20 mm, and the elastic modulus is 3000 MPa.

The reduced steel–concrete contact stiffness of studs increases the local stress concentration of the base metal, as shown in Fig. 7. In the case of push-out test, K_b of the base metal in the rubber sleeved SPJ increases about 13% compared with the stud without rubbers. The results showed that the rubber sleeve relaxes the contact stiffness of studs. This leads to a stress concentration increasing at the toe of the base metal. However, the relaxation of contact stiffness is out of the scope of the NS method. Without further fatigue tests of rubber-sleeved studs, it is difficult to evaluate their fatigue behavior using the NS method.

Although the global NS method is dominant in fatigue evaluation of steel structures, several limitations are discussed in this section. The local HSS method might be an alternative to evaluate the fatigue life of headed studs.

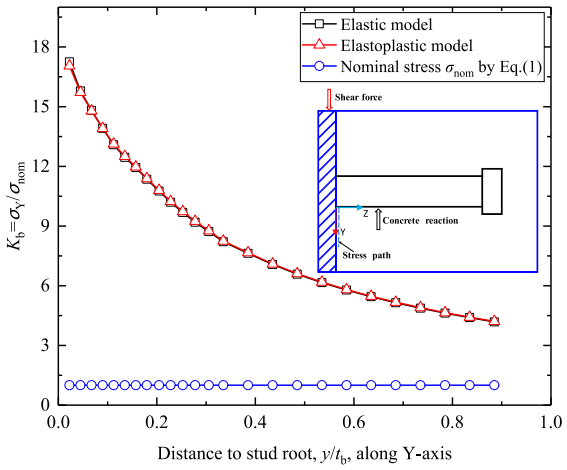

(a) Loading force $P = 40$ kN

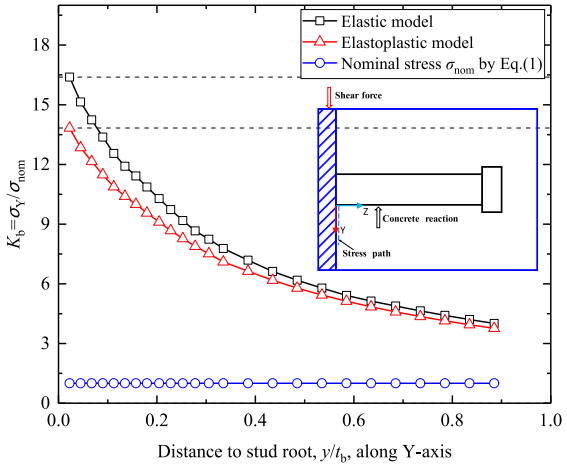

(b) Loading force $P = 100$ kN

Fig. 6. Local stress distribution with material elastoplastic variation.

4.2. Hot spot stress analysis

To determine the HSS of SPJ, the stress extrapolation methods and the finite element modeling techniques are examined. According to the definition of hot spot stress shown in Fig. 8, the linearly extrapolated HSS σ_{hsl} by Eq. (2) and the quadratically extrapolated HSS σ_{hsq} by Eq. (3) are compared in terms of fatigue life prediction. The referring stresses $\sigma_{0.4t}$, $\sigma_{0.9t}$, $\sigma_{1.0t}$ and $\sigma_{1.4t}$ at the top surface of the base plate indicate the normal stresses that are located 0.4 t, 0.9 t, 1.0 t and 1.4 t away from the weld toe, along the Y direction. Where, t is the plate thickness and $t = t_b = 11$ mm for SPJ.

$$\sigma_{hsl} = 1.67\sigma_{0.4t_b} - 0.67\sigma_{1.0t_b} \tag{2}$$

$$\sigma_{hsq} = 2.52\sigma_{0.4t_b} - 2.24\sigma_{0.9t_b} + 0.72\sigma_{1.4t_b} \tag{3}$$

To consider the Poisson's effect on HSS determined by measured strains, the stress σ_{hso} omitting the effect is determined by Eq. (4) and the stress σ_{hsp} including the effect is determined by Eq. (5).

$$\sigma_{hso} = E_s(2.52\varepsilon^y_{0.4t} - 2.24\varepsilon^y_{0.9t} + 0.72\varepsilon^y_{0.9t}) \tag{4}$$

$$\sigma_{hsp} = E_s(2.52(\varepsilon^y_{0.4t} + \nu\cdot\varepsilon^x_{0.4t}) - 2.24(\varepsilon^y_{0.9t} + \nu\cdot\varepsilon^x_{0.9t}) + 0.72(\varepsilon^y_{0.9t} + \nu\cdot\varepsilon^x_{0.4t}))/(1 - \nu^2) \tag{5}$$

where E_s is Young's modulus of steel, and is set to 210GPa. ν is Poisson's ratio of steel and is set to 0.3. The referring strains $\varepsilon^y_{0.4t}$ and $\varepsilon^x_{0.4t}$ represent the normal strain component along the Y-axis and the X-axis, respectively.

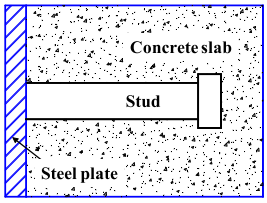

(a) Regular use of studs

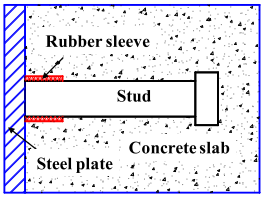

(b) Rubber sleeve studs
(Xu et al. 2014; Xu and Liu 2016)

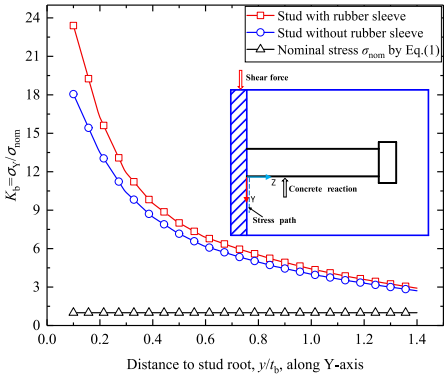

(c) Stress with contact stiffness variation

Fig. 7. Local stress distribution with contact variation.

4.2.1. Effects of mesh size

The referring stresses of HSS are close to the weld toes of SPJ to reflect the local stress concentration. The mesh size may affect local stress distribution. Previous research showed that the multi-sub-model technique might be effective to suppress the computing cost for FE analysis, especially when solid elements are used to predict the steep stress gradient around the stress singularity point [24]. Since the steel–concrete contact in this paper is not covered in previous research on steel structures, the sub-model is checked to verify its accuracy. As shown in Fig. 9, the sub-model is compatible with the global model since they share almost the same stress distribution if using the same mesh intensity. Given the mesh is refined, the much steeper stress distribution in front of the weld toe is obtained by the sub-model. It seems that the multi-sub model is capable to capture the stress peak of SPJ.

Using coarse mesh, the referring stresses vary with mesh size, and refined meshes are required to eliminate its influence, as shown in Fig. 10. Given the mesh size less than 1 mm is applied, the referring stress at 0.4 t away from the weld toe comes to be convergent. About 10% deviation of the stress prediction is suppressed using the refined model. It is recommended that the refined analysis with a tiny element length less than 1 mm may be necessary since the referring stress results are sensitive to the mesh size.

4.2.2. Effects of stress extrapolation

Linear and quadratic stress extrapolation results are checked to evaluate the stress peak at the weld toe, with increasing mesh intensity. As shown in Fig. 11, the quadratic algorithm yields about 14% higher HSS prediction compared with the linear method. The attachment of the welded stud leads to abrupt section change in the base plate. Besides, the push-out force results in concentrated shear force and local bending in SPJ. The quadratic stress extrapolation is favorable to evaluate the non-linear stress gradient induced by structural discontinuity, both geometrically and mechanically. Since the referring stresses come to be convergent using the refined model, the extrapolated results of HSS yield convergence with the mesh size less than 1 mm. The deviation of the non-linear HHS prediction owing to element size is eliminated in this paper.

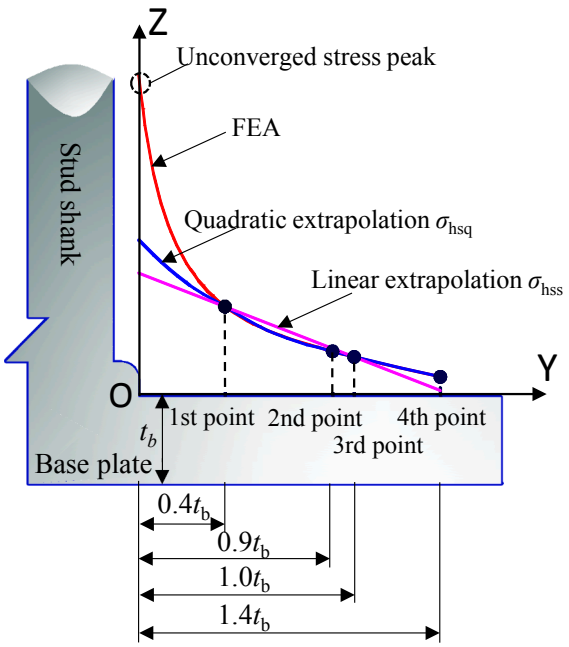

Fig. 8. Hot spot stress of toe-base fatigue.

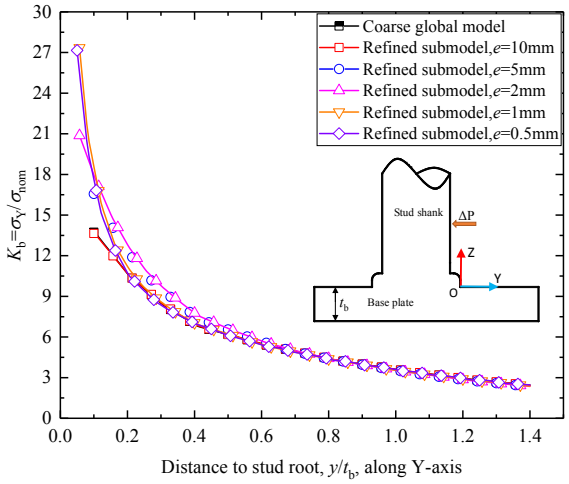

Fig. 9. Verification of sub-modeling with σ_Y along Y axis.

4.2.3. Effects of weld shape

To check the influence on HSS prediction regarding the presence of weld collar, three cases, labeled as a tubular, taper, and without weld collar, are analyzed. As shown in Fig. 12, the tubular weld provides a transition between the stud shank and the base plate, and stress concentration at the weld toe is decreased.

Generally, the ceramic ferrule installed during the drawn-arc welding process of the stud may result in tubular shaped weld collar. Given the stud is welded properly, the model including tubular weld collar may result in a proper HSS prediction. In the process of strength prediction, the gentle HSS and the corresponding fatigue durability may derive a conservative fatigue strength for SPJ. In the process of fatigue evaluation for design purposes, the HSS of a model without weld collar may results in about 26% overestimation than that with tubular-shaped weld collar, as shown in Fig. 13. It ought to yield a conservative design. Nevertheless, the model with the tubular weld collar might be a reasonable alternative if the weld quality is guaranteed.

4.2.4. Effects of toe radius

Like the case in welded steel plates, the toe radius influences on HSS of SPJ. The smaller of toe radius leads to steeper stress distribution shown in Fig. 14, even with the same mesh intensity. HHS using the model with zero toe radius is about 35% lower than

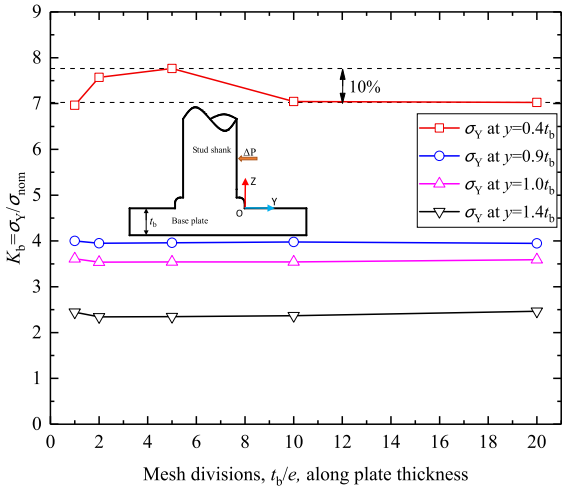

Fig. 10. Stresses at reference points with mesh size variation.

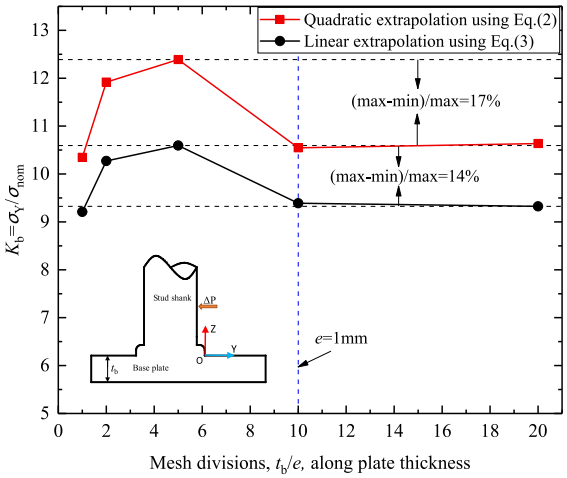

Fig. 11. Hot spot stress with extrapolation variation.

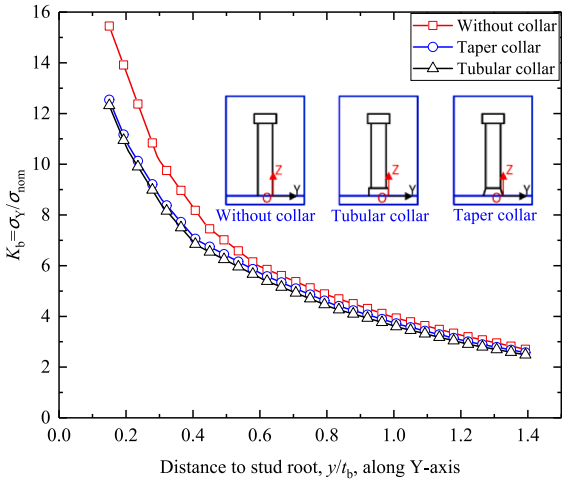

Fig. 12. Local stress distribution with weld shape variation.

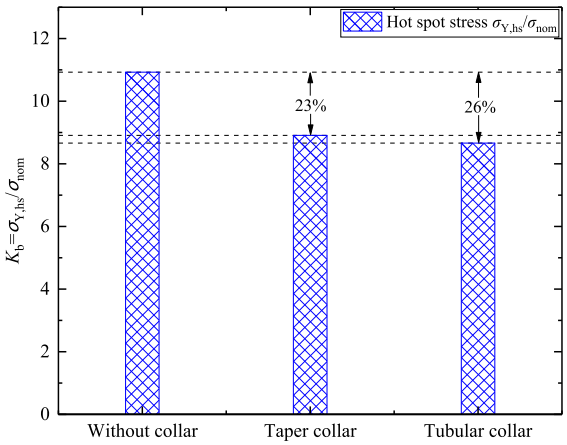

Fig. 13. Hot spot stress with weld shape variation.

that with a 2 mm toe radius, as shown in Fig. 15. In engineering application, after-weld treatment is generally neglected in terms of SPJ, and the smooth weld toe is not expected. Besides, weld beads may splash through the gap between the ceramic ferrules and the base plate. Thus, the weld toe with zero radii might be acceptable. With improved ferrules [13], better weld toe shape can be formed and fatigue behavior might be promoted. In this paper, the fatigue test results from the literature may have different welding quality, and the toe radius is set to zero.

4.3. Prediction of fatigue strength

According to the methodology of HSS, the factors at the structural level, such as member geometry, weld geometry and mesh size, are explicitly included in the FE model. The resistance against HSS at the material level, such as micro-notch defects and residual stress, is determined according to fatigue tests assuming that the welding technique is the same. For general fillet and groove welding used in steel structures, lots of researches proposed to use HSS to determine fatigue strength. However, the drawn arc welding technique is somehow different compared with fillet and groove welding. The fatigue resistance should be determined accordingly.

By applying the derived push-out fatigue loads to FE models with the loads determined according to the nominal shear stresses in the studs, this paper evaluate the efficiency of the HSS method by comparing the prediction and fatigue test results in the literature. In detail, the S-N curve is reconstructed based on FE analysis and HSS methods, and the predicted life is compared against the fatigue tests in the literature.

The least-square method is used to fit the linear regression of the average fatigue strength of the SPJ [19], as shown in Eq. (7):

$$\log(\Delta S) = (k - \log N)/m \tag{7}$$

Lower limit standard fatigue strength curve for 97.7% survival rate, is calculated using Eq. (8):

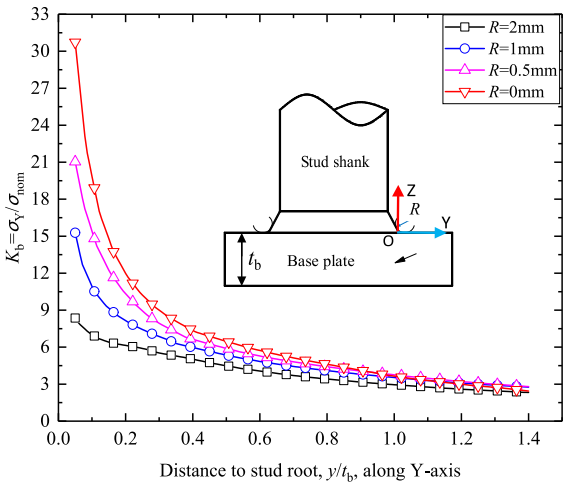

Fig. 14. Local stress distribution with toe radius variation.

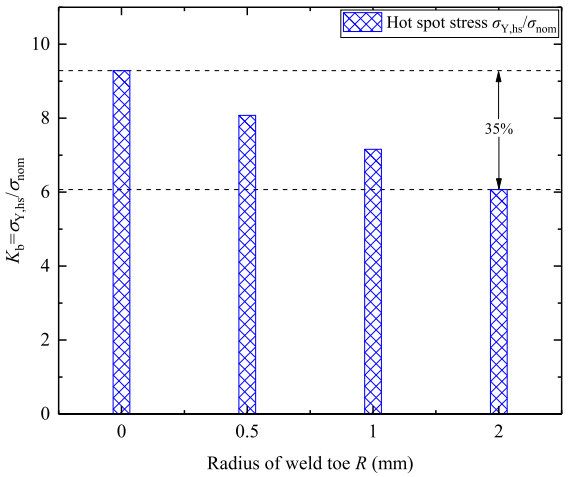

Fig. 15. Hot spot stress with toe radius variation.

$$log(\Delta S^*) = (k - logN)/m - 2\sigma_{log\Delta S} \tag{8}$$

where ΔS, ΔS^* is the hot spot and nominal fatigue stress amplitude respectively; N is the number of cycles of fatigue stress amplitude;$\sigma_{\log\Delta s}$ is the standard deviation.

The fitting curve of fatigue strength based on the NS method is shown in Fig. 16. The fatigue life of the structure is the fatigue strength corresponding to a 2 million cycle life. The average fatigue life fitted by previous tests is FAT102. The fatigue life recommended by JSSC and EC4 codes is FAT80 and FAT95 respectively. Most test results fall within this range, which is suitable for evaluating the fatigue strength of studs by NS amplitude. The fatigue life recommended by AASHTO code is FTA66, which is conservative and more suitable for low cycle fatigue strength.

The fatigue life was evaluated by the HSS amplitude of the SPJ. The fitting curve of the hot spot fatigue strength is shown in Fig. 17. According to different finite element models, the HSS amplitude corresponding to shear fatigue amplitude is obtained. The average hotspot fatigue strength curve is fitted as Eq. (9). The average hot spot fatigue strength of the SPJ is FAT187. The standard fatigue life curve can be obtained by subtracting the average fatigue strength by twice the standard deviation of HSS amplitude ($\sigma_{\log\Delta s} = 0.12$), as shown in Eq. (10).

$$\log\Delta\sigma_{hs} = 3.62 - 0.214\log N \tag{9}$$

$$\log\Delta\sigma_{hs}{}^{*} = 3.38 - 0.214\log N \tag{10}$$

The standard fatigue life obtained by HSS amplitude is FAT107, which is consistent with the fatigue strength FAT90, FAT100 and FAT112 recommended by IIW. The results showed that it is feasible and appropriate to use HSS amplitude to evaluate the fatigue strength of the SPJ of studs.

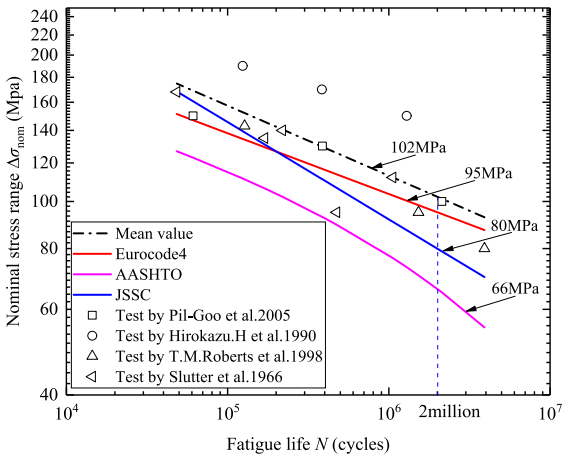

Fig. 16. Fatigue strength of studs based on nominal stress.

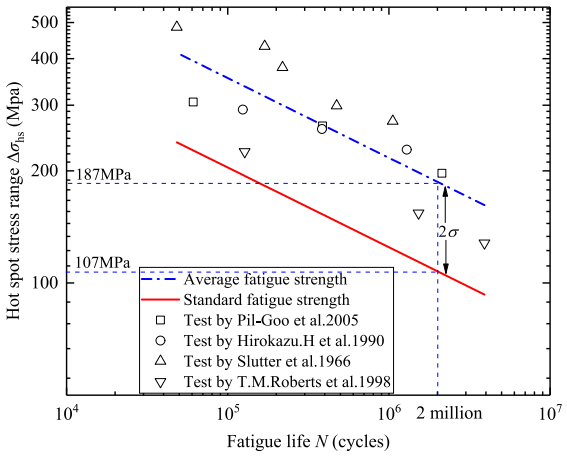

Fig. 17. Fatigue strength of toe-base crack based on hot spot stress.

5. Conclusions

The limitation using the NS method to predict the fatigue life of studs is discussed in this paper. The efficiency of the HSS analysis technique is validated by the fatigue test results in the literature. The main conclusions are as follows:

(1) NS method could not effectively consider the effects of eccentricity, stud spacing, concrete creep, the plasticity of materials, and contact relaxations in the prediction of fatigue life of the headed studs with toe-plate failure mode. HSS method reflects the stress concentration at the weld toe and is able to include the stress variations induced by the above-mentioned effects.
(2) The refined sub-model with less than 1 mm mesh size yields convergent HSS of SPJ and it may be used to predict the HSS of studs together with the quadratic stress extrapolation method.
(3) According to the 100 MPa derived fatigue strength against HSS, SPJ using drawn arc welding shows similar hot spot fatigue strength compared with fillet welding. The derived fatigue strength could be used for further fatigue evaluation on studs with the same welding fabrication technique.

Declaration of Competing Interest

The authors declare that they have no known competing financial interests or personal relationships that could have appeared to influence the work reported in this paper.

Acknowledgements

The research reported herein has been carried out as part of the research projects granted by the National Natural Science Foundation of China (51978245). This paper is also partly supported by Fundamental Research Funds for National Universities (2019B13314) and China Scholarship Council (201906715010).

References

[1] J.H. Ahn, S.H. Kim, Y.J. Jeong, Fatigue experiment of stud welded on steel plate for a new bridge deck system, Steel Compos. Struct. 7 (5) (2007) 391–404.
[2] American Association of State Highway & Transportation Officials (AASHTO), LRFD-Bridge Design Specifications, AASHTO, Washington, DC, 2010.
[3] American Concrete Institute Committee 209 (ACI 209), Guide for Modeling and Calculating Shrinkage and Creep in Hardened Concrete, Michigan, 2008.
[4] ANSYS, Release 14.0. ANSYS University Advanced, ANSYS Inc., 2013.
[5] S. Chen, Y. Huang, P. Gu, J.Y. Wang, Experimental study on fatigue performance of UHPC-orthotropic steel composite deck, Thin-Wall. Struct. 142 (2019) 1–18.
[6] E. Ellobody, B. Young, Performance of shear connection in composite beams with profiled steel sheeting, J. Constr. Steel Res. 62 (7) (2006) 682–694.
[7] European Committee for Standardization, Eurocode 3: Design of Steel Structures-Part 1-9: Fatigue, Brussels, EN 1993-1-9, 2005.
[8] European Committee for Standardization, Eurocode 4: Design of Composite Steel and Concrete Structures-Part 1.1: General Rules and Rules for Buildings, Brussels, EN 1994-1-1, 2004.
[9] W. Fricke, D.D. Tchuindjang, Fatigue strength behavior of stud-arc welded joints in load-carrying ship structures, Weld. World 57 (4) (2013) 495–506.
[10] G. Hanswille, M. Porsch, C. Ustundag, Resistance of headed studs subjected to fatigue loading: Part I: Experimental study, J. Constr. Steel Res. 63 (4) (2007) 475–484.
[11] J. He, S. Wang, Y. Liu, D. Wang, H. Xin, Shear behavior of steel I-girder with stiffened corrugated web, part II: Numerical study, Thin-Wall. Struct. (2019).
[12] S. He, Z. Fang, A.S. Mosallam, Y. Ouyang, C. Zou, Behavior of CFSC-encased shear connectors in steel-concrete joints: Push-out tests, J. Struct. Eng. 146 (4) (2020) 04020015.
[13] H. Higashiyama, K. Yoshida, K. Inamoto, S. Matsui, H. Kaido, Fatigue of headed studs welded with improved ferrules under rotating shear force, J. Constr. Steel Res. 92 (2014) 211–218.
[14] J. Hildebrand, H. Soltanzadeh, A review on assessment of fatigue strength in welded studs, Int. J. Steel Struct. 14 (2) (2014) 421–438.
[15] H. Hirokazu, Study on the fatigue strength and static design method of headed stud, Ph.D. dissertations, Osaka University, Osaka, 1990 (In Japanese).

[16] A. Hobbacher, Recommendations for Fatigue Design of Welded Joints and Components, Springer, Switzerland, 2016.
[17] Japanese Society of Steel Construction (JSSC), Fatigue Design Recommendations for Steel Structures, Tokyo, 2012 (in Japanese).
[18] JTG D64 2015, Steel Bridge Design Specifications, Beijing, China, 2015 (in Chinese).
[19] R.P. Johnson, Resistance of stud shear connectors to fatigue, J. Constr. Steel Res. 56 (2000) 101–116.
[20] K. Liu, G.D. Roeck, Parametric study and fatigue-life-cycle design of shear studs in composite bridges, J. Constr. Steel Res. 65 (5) (2009) 1105–1111.
[21] Y.X. Li, Y. Liu, R. Liu, Finite element analysis on axial compressive behaviors of high-performance steel stiffened plates in bridge application, Int. J. Steel Struct. 19 (2019) 1624–1644.
[22] Y. Liu, H. Xin, J. He, D. Xue, B. Ma, Experimental and analytical study on fatigue behavior of composite truss joints, J. Constr. Steel Res. 83 (2013) 21–36.
[23] Y. Liu, H. Xin, Y. Liu, Load transfer mechanism and fatigue performance evaluation of suspender-girder composite anchorage joints at serviceability stage, J. Constr. Steel Res. 145 (2018) 82–96.
[24] R. Liu, Y. Liu, B. Ji, M. Wang, Y. Tian, Hot spot stress analysis on rib–deck welded joint in orthotropic steel decks, J. Constr. Steel Res. 97 (2014) 1–9.
[25] P.G. Lee, C.S. Shim, S.P. Chang, Static and fatigue behavior of large stud shear connectors for steel–concrete composite bridges, J. Constr. Steel Res. 61 (2005) 1270–1285.
[26] J.G. Nie, M.X. Tao, L.L. Wu, X. Nie, F.X. Li, F.L. Lei, Advances of research on steel-concrete composite bridges, China Civil Eng. J. 45 (6) (2012) 110–122 (in Chinese).
[27] J.G. Nie, Y.H. Wang, Research status on fatigue behavior of steel-concrete composite beams, Eng. Mech. 29 (6) (2012) 1–11 (in Chinese).
[28] H.T. Nguyen, S.E. Kim, Finite element modeling of push-out tests for large stud shear connectors, J. Constr. Steel Res. 65 (2009) 1909–1920.
[29] T.M. Roberts, O. Dogan, Fatigue of welded stud shear connectors in steel–concrete–steel sandwich beams, J. Constr. Steel Res. 45 (3) (1998) 301–320.
[30] R.G. Slutter, J.W. Fisher, Fatigue strength of shear connectors, Highway Res. Rec. 147 (1966) 65–88.
[31] C.O. Viana, H. Carvalho, José Correia, P.A. Montenegro, Rui Calçada, Fatigue assessment based on hot-spot stresses obtained from the global dynamic analysis and local static sub-model, Int. J. Structural. Integr. (2019), https://doi.org/10.1108/IJSI-03-2019-0021.
[32] H. Xin, M. Nijgh, M. Veljkovic, Computational homogenization simulation on steel reinforced resin used in the injected bolted connections, Compos. Struct. 210 (2019) 942–957.
[33] H. Xin, M. Veljkovic, Effects of residual stresses on fatigue crack initiation of butt-welded plates made of high strength steel, in: Proceedings of the Seventh International Conference on Structural Engineering, Mechanics and Computation (SEMC 2019), Cape Town, South Africa, 2019, pp. 2–4.
[34] H. Xin, M. Veljkovic, Residual stress effects on fatigue crack growth rate of mild steel S355 exposed to air and seawater environments, Mater. Des. (2020) 108732.
[36] X. Xu, Y. Liu, Analytical and numerical study of the shear stiffness of rubber-sleeved stud, J. Constr. Steel Res. 123 (2016) 68–78.
[37] X. Xu, Y. Liu, J. He, Study on mechanical behavior of rubber-sleeved studs for steel and concrete composite structures, Constr. Build. Mater. 53 (2014) 533–546.
[38] D. Xue, Y. Liu, Z. Yu, J. He, Static behavior of multi-stud shear connectors for steel-concrete composite bridge, J. Constr. Steel Res. 74 (8) (2012) 1–7.
[39] Z.Y. Zhou, F. Li, Study on fatigue analysis of welded toes of plate structures using hot spot stress method based on surface extrapolation, J. Railw. 31 (5) (2009) 90–96 (in Chinese).
[40] R. Liu, Z. Feng, H. Ye, Y. Liu, Stress redistribution of headed stud connectors subjected to constant shear force, Int. J. Steel Struct. 20 (2020) 436–451, https://doi.org/10.1007/s13296-019-00295-3.